*Desalination and Water Treatment*
www.deswater.com

1944-3994/1944-3986 © 2013 Balaban Desalination Publications. All rights reserved
doi: 10.1080/19443994.2012.734734

51 (2013) 2014–2020
February

Taylor & Francis
Taylor & Francis Group

# Adsorption and kinetic studies of cesium ions from aqueous solution by functionalized silica

Rajesh Kumar, Surendra Kumar Jain*

*Water Quality Management Group, Desert Environmental Science and Technology Division, Defence Laboratory, Ratanada Palace, Jodhpur, 342011 Rajasthan, India*
*Tel. +91-291-2567510; email: skj_dl97@rediffmail.com*

Received 23 March 2011; Accepted 30 August 2012

## ABSTRACT

In this work, functionalized silica (F-silica) was synthesized by condensation reaction of 2-hydroxyacetophenone-3-thiosemicarbazone with diazotized silica and evaluated for removal of cesium ion from aqueous solution. The synthesized compound was characterized using Fourier transform-infrared spectroscopy. The batch experiments were carried out in a range of initial cesium concentration from 500 to 2,500 μg/L using F-silica in the solution. The effect of initial cesium concentration and contact time on process kinetics and equilibrium were also studied. Nonradioactive cesium chloride was used as a surrogate of the radioactive cesium. The experimental data were analyzed using equilibrium isotherm Freundlich and Langmuir models. The adsorption data were well described by Freundlich model. Pseudo-first-order and pseudo-second-order kinetic models were used to analyze the adsorption-rate data. The pseudo-second-order model was found to correlate best with the kinetic data. The results showed that F-silica can adsorb Cs(I) with high efficiency by chemisorption and physiosorption mechanisms.

*Keywords:* Adsorption isotherm; Adsorption kinetics; Cesium metal ion; Functionalized silica; Radioactive nuclides

## 1. Introduction

The heavy metal ions are toxic or carcinogenic and hence present a threat to human health and the environment, when they exist in or are discharged into various water resources. These metal ions are present in wastewater discharge of many industries among which the plating facilities, batteries, alloys, electroplated metal parts, mining, refining and production of textiles, paints and dyes operations are easily distinguishable due to their severe environmental impacts and ever-present risks associated with mismanagement [1,2]. Nowadays, the major problem is contamination of the water with long-lived radionuclides such as cesium, strontium, lanthanides, and actinides. The main sources of radioactive wastes are operation of nuclear power plants, research facilities, and the use of radioisotopes in industry and diagnostic medicine [3–6]. During the nuclear war and mismanagement of nuclear power reactors, drinking water was contaminated with radionuclides and their degraded products. The nuclear war and mismanagement of nuclear power reactors has already taken place at different times such that water is contaminated with radioactive iodine and cesium after an explosion at a nuclear power plant due to the great east Japan earthquake. Recently, drinking water contaminated with radionuclides has become an emerging threat to military as well as civilian population. Therefore, the removal of

---

*Corresponding author.

radionuclides from contaminated water is a necessary requirement.

Several technologies such as thermal treatment, precipitation, filtration, evaporation, nanofiltration, ion exchange using organic resins, and adsorption [7–9] have been proposed to treat radioactive waste. Among these techniques, adsorption is one of the most promising processes and many types of adsorbents have been applied including modified alumina, $TiO_2$ (Anatase and Rutile), attapulgite [10–12], synthetic inorganic material [13,14], modified zeolites [15], bentonite [16], polyacrylamide cerium titanate polymer [17], and titanium tungstate [18]. However, the organic resins and other adsorbents have a drawback due their ability to swell and low-removal efficiency.

The adsorptions of radionuclides on other materials such as carbon nanotubes [19,20] and cement mortar [21] have been studied. Nonmodified carbon nanotubes show insufficient adsorption efficiency due to their poor-dispersion property. Therefore, researchers carried out investigation for new promising adsorbents [22]. Among the different adsorbents, silica gel, especially immobilized with various organic compounds with metal-chelating functionality, has received great attention [23]. Silica has various advantages over other organic/inorganic supports such as: immobilization is easier on silica surface than on organic polymeric supports, high specific surface area [24] high mass exchange characteristics and no swelling, great resistance to organic solvents [25], and very high thermal resistance [26]. In this context, a search for newer adsorbent is essential. The adsorption approach involving application of F-silica in removal of cesium from the waste water can offer a complete solution.

Our laboratory has developed various water purification technologies for wastewater treatment [27]. Now our research and development is focusing on developing a novel adsorbent for removal of radionuclides from contaminated water. The objective was to find the optimum conditions for the removal of Cs (I) from contaminated water under different treatment conditions such as contact time, dose, pH, and initial concentration.

In this paper, F-silica has been prepared by the condensation reaction of diazotized 3-aminopropyl silica with 2-hydroxyacetophenone-3-thiosemicarbazone. After characterization, it was evaluated for the removal of Cs(I) ions from aqueous solution and adsorption kinetics parameters were also calculated. To our best knowledge, the use of such material for the removal of Cs(I) ions has not been reported.

## 2. Experimental

### 2.1. Instrumentation

Metal-ion removal studies were carried out by using atomic absorption spectrometer (AAS) (Analytik-Jena-Nova-400) on flame mode with single beam. AAS equipped with 100 mm burner, a cross flow nebulizer 5.0 mL/min, and 1.2 mm slit were used throughout the experiments. Each experiment was duplicated under identical conditions using this instrument for concentration determination. IR spectra of the compound were recorded on Jasco fourier transform-infrared spectroscopy (FT-IR) model 610 by using KBr pellets. The pH measurements were made on a digital pH meter (HACH, sension 1, model 51935-00) equipped with a gel-filled pH electrode. The meter was calibrated with the buffers of 4, 7, and 10.

### 2.2. Chemicals and solutions

All the reagents used during experiments were of analytical-grade. All laboratory wares used for analytical determination were cleaned first by nitric acid and hydrochloric acid, followed by repeated rinsing with de-ionized water. All the solutions were prepared with ultrapure water (resistivity: 18.2 MΩ cm) from an Elix analytical reagent-grade water purification system. 3-Aminopropyl silica was purchased from Aldrich with characteristics of particle platform irregular, functionalized 9%, surface area $550\,m^2/g$ and mean pore size 60 Å.

Calibration standard solutions and internal standards were prepared from commercial metal standard solutions. Analytical grade nitric acid (Fisher) was used as acid for the preparation of all the calibration standard solutions and analytical solutions. Standard working solutions 1,000 mg/L of cesium were prepared from CsCl Suprapur$^R$ (Merck, Germany) and solutions of varying initial concentrations were prepared from the 1,000 mg/L solution by serial dilution, using distilled deionized water.

### 2.3. Functionalization of 3-aminopropyl silica with 2-hydroxyacetophenone-3-thiosemicarbazone

#### 2.3.1. Synthesis of 2-hydroxyacetophenone-3-thiosemicarbazone

2-Hydroxy acetaphenone (0.3 mol dissolved in 50 mL of methanol), thiosemicarbazide (0.3 mol dissolved in 200 mL of water) and potassium hydroxide (3 g dissolved in 25 mL of water) were mixed in a round bottomed flask and refluxed for 3 h and after cooling the mixture, was poured in ice water. The yellow crystals obtained were washed with ethanol and recrystallized in ethanol (Scheme 1).

3-Aminopropyl silica (10 g) and 20 mL HCl solution (conc. HCl:$H_2O$; 1:1 v/v) were stirred in conical flask at 0–4˚C. To this, drop wise solution of 10 mL $NaNO_2$ (5 M solution of $NaNO_2$ in water) was added until the reaction mixture showed a permanent dark blue color with starch-iodine paper with continuous stirring. The diazotized silica was washed with ice-cold water and reacted with 2-hydroxyacetophenone-3-thiosemicarbazone (2 g dissolved in 50 mL of 10% NaOH solution) at 0–4˚C for 10 h. The resulting product was filtered, washed with water, and dried (Scheme 2).

### 2.4. Adsorption studies with batch method

Batch adsorption experiments were carried out in glass bottles (100 mL) containing F-silica (50 mg) with 10 mL of Cs(I) ions of desired concentration at 30 ± 1˚C. The bottles were shaken for 5–30 min and solutions containing Cs(I) ions were filtered using Whatman filter paper (No. 42). After each experiment, the residual concentration of Cs(I) ions was determined by AAS. The amount of metal ion adsorbed by F-silica ($Q_e$ mmol/g) was calculated according to the following equation:

$$Q_e = (C_i - C_e) \times V/m \qquad (1)$$

where $C_i$ and $C_e$ are initial and equilibrium concentration (μg/L), respectively. $V$ (L) and $m$ (g) are volume of the sample solution and mass of the F-silica. The observed adsorption data were fitted with Langmuir and Freundlich models.

### 2.5. Kinetic adsorption experiment

The kinetic study was carried out at two concentrations (1,000 and 2,000 μ/L) at pH 7. Data acquisition protocol includes the treatment of a series of 50 mg of the F-silica with 10 mL of cesium solution. These series of samples are quenched at time interval by filtration. The concentrations of the filtrate were analyzed by AAS. These results were also used to obtain the adsorption kinetics.

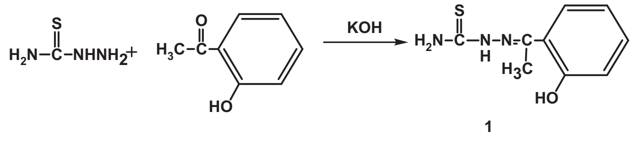

Scheme 1. Synthesis of 2-hydroxyacetophenone-3-thiosemicarbazone.

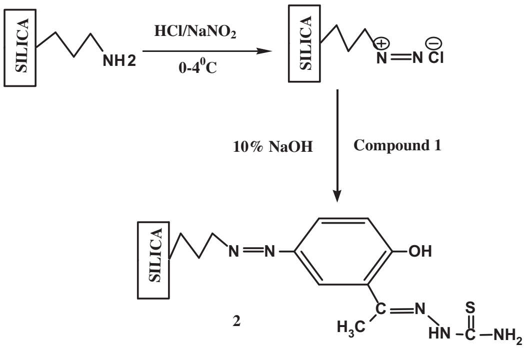

Scheme 2. Functionalization of 3-aminopropyl silica with 2-hydroxyacetophenone-3-thiosemicarbazone.

## 3. Results and discussion

### 3.1. Characterization of functionalized silica

A schematic representation of synthesis of 2-hydroxyacetophenone-3-thiosemicarbazone (1) is shown in Scheme 1. The FT-IR spectrum of 2-hydroxyacetophenone-3-thiosemicarbazone (Fig. 1) showed absorption bands at 3,420, 3,250, 1,623, 1,376, 1,240, and 1,106 $cm^{-1}$ due to $NH_2$ stretching, O–H stretching, C = N stretching, C = S stretching, O–H bending and C–N stretching [28], respectively. The appearance of the characteristic IR absorption bands of these groups is a proof for the compound 1.

The synthesized compound was used to functionalize 3-aminopropyl silica as shown in Scheme 2.

FT-IR of 3-aminopropyl silica (Fig. 2(a)) shows absorption band at 1,150 $cm^{-1}$ for the Si–O–Si group and O–H stretching of silanol group at 3,450 $cm^{-1}$. After functionalization with compound 1 new

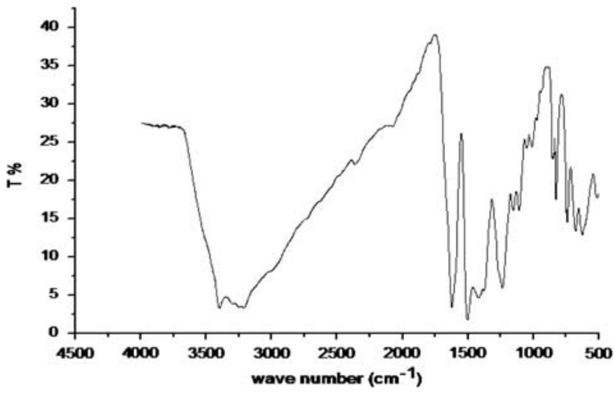

Fig. 1. FT-IR spectra of functionalized 2-hydroxyacetophenone-3-thiosemicarbazone (Compound 1).

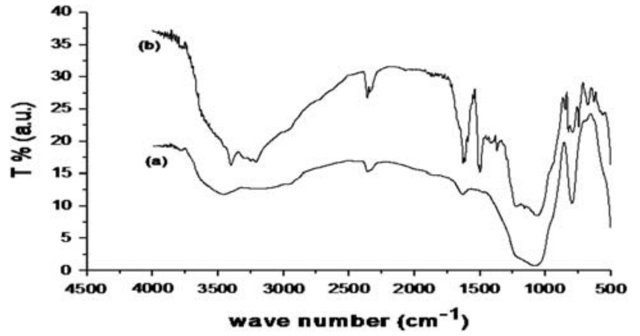

Fig. 2. Comparative FT-IR spectra of (a) 3-aminopropyl silica (b) F-silica with 2-hydroxy acetaphenone-3-thiosemicarbazone.

absorption bands (Fig. 2(b)) appear at 3,436, 1,670, 1,525, 1,390, 1,230 and 1,105 $\mathrm{cm}^{-1}$ which may be assigned to $NH_2$ stretching, C = N stretching, N = N stretching, O–H bending, C = S stretching and C–N stretching, respectively, and the presence of Si–O–Si group absorption band at 1,150 $\mathrm{cm}^{-1}$[29]. The presence of absorption band of these groups confirmed that 3-aminopropyl silica functionalized with 2-hydroxy-acetophenone-3-thiosemicarbazone.

### 3.2. Adsorption isotherm

The adsorption isotherm of Cs(I) onto F-silica from aqueous solution has shown that the adsorption capacity of Cs(I) onto F-silica increases with increasing the initial Cs(I) concentration, increases and continues up to 2,000 μg/L and levels off thereafter. The initial Cs(I) concentrations (500, 1,000, 1,500, 2,000 and 2,500 μg/L) have been used for investigation of the adsorption isotherm. The equilibrium concentrations are obtained after 10 min of contact time.

Langmuir [30] and Freundlich [31] models are employed to describe the adsorption process.

The Langmuir isotherm (Fig. 3) model is given as

$$C_e/Q_e = 1/(q_m b) + C_e/Q_m \tag{2}$$

where $C_e$ is the equilibrium concentration obtained from the initial concentration upon a certain period of contact time with the F-silica, $Q_e$ is the amount of Cs (I) adsorbed per gram of F-silica (μg/g) at equilibrium, and $Q_m$ is the maximum adsorption capacity (μg/g). $b$ is the Langmuir parameter related to energy of adsorption. $Q_e$ is derived from the Eq. (1). The linear plot of $C_e/Q_e$ vs. $C_e$ gives the intercept and slope corresponding to $1/(Q_m b)$ and $1/Q_m$, respectively, from which both $Q_m$ and $b$ are derived. A plot of $C_e/Q_e$ vs. $C_e$ obtained a straight line if the Langmuir equation is obeyed by the adsorption equilibrium [32].

Freundlich isotherm (Fig. 4) can be expressed as

$$\log Q_e = 1/n \ \log C_e + \log K \tag{3}$$

where $K$ and $1/n$ are Freundlich constants, indicating the sorption capacity and sorption intensity, respectively. $C_e$ is the equilibrium concentration of Cs(I) in aqueous solution and $Q_e$ is the sorption capacity. The plot of log$Q_e$ against log $C_e$ gave the intercept and slope corresponding to log $K$ and $1/n$, respectively, from which both $K$ and $n$ are obtained.

The regression equation parameters $Q_m$, $K$, $1/n$, and the correlation coefficient are summarized in Table 1. It is seen that the Freundlich model is more suitable to fit the adsorption data than Langmuir model, since the correlation coefficients are higher than 0.99. The numerical value of $1/n < 1$ indicates that adsorption is fitted to Freundlich model and multilayer adsorption on the surface.

### 3.3. Adsorption kinetics

The kinetic property of Cs(I) adsorbed on the F-silica was assessed (Fig. 5). The adsorption rates were determined at pH 7 in the range of Cs(I) concentrations 1,000 and 2,000 μg/L in aqueous solution. It is

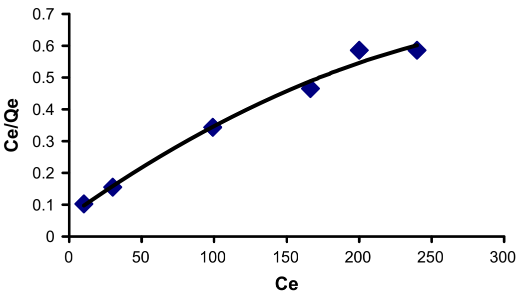

Fig. 3. Langmuir isotherm of Cs(I) adsorption onto F-silica.

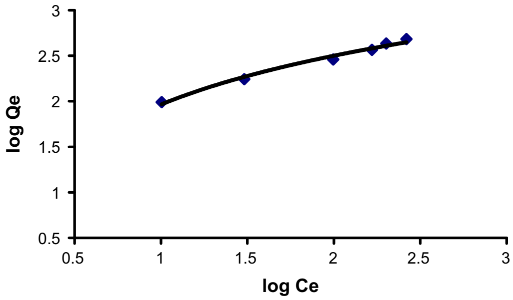

Fig. 4. Freundlich isotherm of Cs(I) adsorption onto F-silica.

Table 1
Langmuir and Freundlich parameters of Cs(I) adsorption

| Langmuir model | | | Freundlich model | | |
|---|---|---|---|---|---|
| $Q_m$(μg/g) | $b$(L/μg) | $R^2$ | $K$ | $1/n$ | $R^2$ |
| 370 | 0. 0039 | 0.9613 | 0.1760 | 0.4369 | 0.9992 |

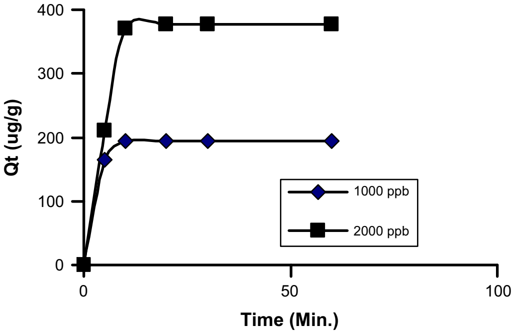

Fig. 5. The adsorbed amounts of Cs(I) at different time intervals.

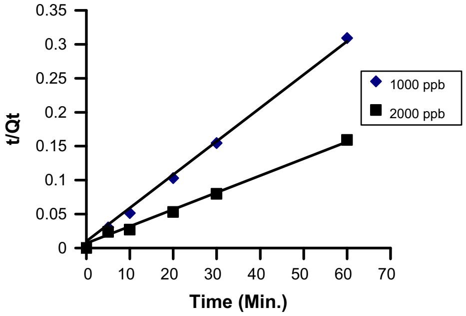

Fig. 6. Second-order kinetic plot for the adsorption of Cs(I) ions.

observed that the adsorption increases with increased concentration of the metal ion. At any given concentration, the Cs(I) adsorption quickly rose, and then reached the plateau, which is the equilibrium capacity.

The adsorption data will be applied to selected adsorption kinetic models, namely the pseudo-first-order and pseudo-second-order equations [33]. The pseudo-second-order reaction is expressed as [34]:

$$t/Q_t = 1/(k_2 Q_e)^2 + t/Q_e \qquad (4)$$

where $Q_e$ (μg/g) is the amount of metal ion adsorbed at equilibrium, $Q_t$ (μg/g) is the amount of metal ion on the surface of the sorbent at time $t$ and $k_2$ [g/(μg min)] is the rate constant of pseudo-second-order adsorption. The values of $1/(k_2 Q_e)^2$ and $1/Q_e$ are derived experimentally from the intercept and slope of the linear plots of $t/Q_t$ vs. $t$, which eventually leads to values of $k_2$ and $Q_e$ (Fig. 6).

The kinetic parameters for the adsorption of Cs(I) onto F-silica are summarized in Table 2. An analysis of the data in Table 2 indicates that the correlation coefficient $R^2$, of the pseudo-first-order model at initial concentration (1,000, 2,000 μg/L) did not exceed the value of 0.6320 and $Q_e$ value is too low. This shows that the adsorption of Cs(I) by F-silica did not follow the pseudo-first-order reaction. The correlation coefficient $R^2$ of the pseudo-second-order model is extremely high (greater than 0.995) and $Q_e$ value is also too high.

Table 2
Kinetic parameters for Cs(I) adsorption onto the F-silica

| | | | |
|---|---|---|---|
| Pseudo-second-order | | | |
| $C_0$ (μg/L) | $K_2$ [g/(min μg)] | $Q_e$ (μg/g) | $R^2$ |
| 1,000 | $5.3404 \times 10^{-2}$ | 187.235 | 0.997 |
| 2,000 | $3.14 \times 10^{-2}$ | 380.571 | 0.995 |
| Pseudo-first-order | | | |
| $C_0$ (μg/L) | $K_2$ (1/min) | $Q_e$ (μg/g) | $R^2$ |
| 1,000 | $3.1076 \times 10^{-7}$ | 9.378 | 0.3172 |
| 2,000 | $1.0945 \times 10^{-7}$ | 14.064 | 0.6320 |

It is found that pseudo-second-order model is applicable to the present adsorption kinetics of Cs(I).

## 4. Conclusions

F-silica was successfully prepared by condensation reaction of diazotized 3-aminopropyl silica with 2-hydroxyacetophenone-3-thiosemicarbazone and characterized by FT-IR. The adsorption of Cs(I) ions on functionalized silica was investigated by the batch method. The effect of parameters on removal of Cs(I) from aqueous solution were also studied. The equilibrium data were analyzed using Freundlich and Langmuir isotherms. The Freundlich model was demonstrated to provide the best correlation constant 0.995 of cesium adsorption onto F-silica. The maximum adsorption capacity was determined to be 370 μg/g for cesium ions. The kinetic studies revealed that the adsorption process of cesium ions followed well the pseudo-second-order kinetic model. The present study showed that F-silica can be used as a novel adsorbent for removal of radioactive Cs(I) ions from contaminated water.

## References

[1] J.W. Patterson, Industrial Wastewater Treatment Technology, second ed., Butterworth-Heinemann, London, 1985.

[2] J. Roberts, Metal Toxicity in Children in: Training Manual on Pediatric Environmental Health: Putting it into Practice, Children's Environmental Health Network, San Francisco, CA, 1999.

[3] R.V. Kemp, D.G. Bennett, M. White, Recent trends and developments in dialogue on radioactive waste management: Experience from the UK, J. Environ. Int. 32 (2006) 1021–1032.

[4] C. Andrade, I. Martinez, M. Castellote, P. Zuloaga, Some principles of service life calculation of reinforcements and *in situ* corrosion monitoring by sensors in the radioactive waste containers of El Cabril disposal (Spain), J. Nucl. Mater 358 (2006) 82–95.

[5] I. Plecas, S. Dimovic, Curing time effect on compressive strength and incremental leaching rates of $^{137}$Cs and $^{60}$Co in cement immobilized sludge, Prog. Nucl. Eng. 48 (2006) 629–633.

[6] G. Melville, S.F. Liu, B. Allen, A theoretical model for the production of Ac-225 for cancer therapy by photon-induced transmutation of Ra-226, J. Appl. Radiat. Isot. 64 (2006) 979–988.

[7] M.W. Abdel Raouf, Potassium hexacyanocobalt ferrate and ammonium molybdophosphate sorption bags for the removal of $^{137}$Cs from aqueous solutions and a simulated waste, J. Chem. Technol. Biotechnol. 79 (2003) 22–29.

[8] X. Wang, D. Xu, L. Chen, X. Tan, X. Zhou, A. Ren, C. Chen, Sorption and complexation of Eu(III) on alumina: effects of pH, ionic strength, humic acid and chelating resin on kinetic dissociation study, J. Appl. Radiat. Isot. 64 (2006) 414–421.

[9] M.G. Khedr, Nanofiltration and low energy reverse osmosis in rejection of radioactive isotopes and heavy metal cations from drinking water sources, Desalin. Water Treat. 2 (2009) 342–350.

[10] X.L. Tan, X.K. Wang, H. Geckeis, T.H. Rabung, Sorption of Eu(II) on humic acid of fulvic acid bound to hydrous alumina studies by SEM-EDS, XPS, TRLFS and batch techniques, Environ. Sci. Technol. 42 (2008) 6532–6537.

[11] X.L. Tan, Q.H. Fan, X.K. Wang, B. Grambow, Eu(III) sorption to $TiO_2$ (anatase and rutile): Batch, XPS, and EXAFS studies, Environ. Sci. Technol. 43 (2009) 3115–3121.

[12] Q.H. Fan, X.L. Tan, J.X. Li, X.K. Wang, W.S. Wu, G. Montavon, Sorption of Eu(III) on attapulgite studied by batch, XPS, and EXAFS techniques, Environ. Sci. Technol. 43 (2009) 5776–5782.

[13] M. Nilchi, N. Ghanadi, A. Khanchi, Characteristics of novel types of substituted cerium phosphates, J. Radioanal. Nucl. Chem. 245 (2000) 589–594.

[14] G.M. Ibrahim, B. EI-Gammal, I.M. EI-Naggar, Selectivity modification of some alkali metal ions on silicon antimonite as cation exchanger, Curr. Top. Colloid Interf. Sci. 6 (2003) 159–165.

[15] E.H. Borai, R. Harjula, L. Malien, A. Paajanen, Efficient removal of cesium from low-level radioactive liquid waste using natural and impregnated zeolite minerals, J. Hazard. Mater. 172 (2009) 416–422.

[16] Z. Klika, L. Kraus, D. Vopalka, Cesium uptake from aqueous solutions by bentonite: A comparison of multicomponent sorption with ion-exchange models, Langmuir 23 (2007) 1227–1233.

[17] C. Chen, J. Hu, D. Xu, X. Tan, Y. Meng, X. Wang, Surface complexation of Sr(II) and Eu(II) adsorption onto oxidized multi carbon nanotubes, J. Coll. Interf. Sci. 323 (2008) 33–41.

[18] G.M. Ibrahim, Removal of $^{60}$Co and $^{134}$Cs radionuclides from aqueous solution using titanium tungstate ion exchanger, Desalin. Water Treat. 13 (2010) 418–426.

[19] D. Shao, Z. Jing, X. Wang, J. Li, Y. Meng, Plasma induced grafting carboxymethyl cellulose on multiwalled carbon nanotubes for the removal of $UO_2^{+2}$ from aqueous solution, J. Phys. Chem. Lett. 113 (2009) 860–864.

[20] I.M. EI-Naggar, G.M. Ibrahim, E.A. EI-Kady, E.A. Hegazy, Sorption mechanism of $Cs^+$, $Co^{2+}$ and $Eu^{3+}$ ions onto EGIB sorbent, Desalination 237 (2009) 147–154.

[21] K. Volchek, M.Y. Miah, W. Kung, Z. DeMaleki, F.H. Tezel, Adsorption of cesium on cement mortar from aqueous solutions, J. Hazard. Mater. 194 (2011) 331–337.

[22] G.P. Rao, C. Lu, F. Su, Sorption of divalent metal ions from aqueous solution by carbon nanotubes: A review, Sep. Purif. Technol. 58 (2007) 224–231.

[23] B. Anilan, T. Gedikbey, S.T. Akar, Determination of copper in water samples after solid-phase extraction using dimethylglyoxime-modified silica, Clean-Soil, Air, Water 38 (4) (2010) 344–350.

[24] L.N.H. Arakaki, L.M. Nunes, J.A. Simoni, C. Airoldi, Ethyleneimine anchored on thiol-modified silica gel surface-adsorption of divalent cations and calorimetric Data, J. Colloid Interf. Sci. 228 (2000) 46–51.

[25] C.C. Chen, J.S. Do, Y. Gu, Immobilization of HRP in mesoporous silica and its application for the construction of polyaniline modified hydrogen peroxide biosensor, Sensors 9 (2009) 4635–4642. doi: 10.3390/s90604635.

[26] G.Z. Fang, J. Tan, X.P. Yan, An ion-imprinted functionalized silica gel sorbent prepared by a surface imprinting technique combined with a sol−gel process for selective solid-phase extraction of Cadmium(II), Anal. Chem. 77(6) (2005) 1734–1741. doi: 10.1021/ac048570v

[27] R.K. Misra, S.K. Jain, P.K. Khatri, Iminodiacetic acid functionalized cation exchange resin for adsorptive removal of Cr(VI), Cd(II), Ni(II) and Pb(II) from their aqueous solutions, J. Hazard. Mater. 185 (2011) 1508–1512.

[28] G.P.C. Rao, K. Seshaiah, Y.K. Rao, M.C. Wang, Solid phase extraction of Cd, Cu and Ni from leafy vegetables and plant leaves using amberlite XAD-2 functionalized with 2-hydroxy-acetophenone-thiosemicarbazone (HAPTSC) and determination by inductively coupled plasma atomic emission spectroscopy, J. Agric. Food Chem. 54 (2006) 2868–2872.

[29] P.K. Jal, S. Patel, B.K. Mishra, Chemical modification of silica surface by immobilization of functional groups for extractive concentration of metal ions, Talanta 62 (2004) 1005–1028.

[30] I. Langmuir, The constitution and fundamental properties of solids and liquids, J. Am. Chem. Soc. 38 (1916) 2221–2295.

[31] H.M.F. Freundlich, Über die adsorption in läsungen [Over the adsorption in solution], Zeitschrift für Physikalische Chemie [J. Phys. Chem.] 57 (1906) 385–470.

[32] S. Gupta, B.V. Babu, Utilization of waste product (tamarind seeds) for the removal of Cr(VI) from aqueous solution: Equlibrium, kinetics and regeneration studies, J. Environ. Man. 90 (2009) 3013–3022.

[33] Y.S. Ho, G. McKay, The kinetic of sorption of divalent metal ions onto sphagnum moss peat, Water Res. 34 (2000) 735–742.

[34] J.A. Allen, D.A. Brown, Isotherm analyses for single component and multi component metal sorption onto lignite, J. Chem. Technol. Biotechnol. 62 (1995) 17–24.